ELSEVIER

Intercalation of WF_6 in the interlayer space of multiwall carbon nanotubes—structural and morphological aspects

D. Claves[a],*, J. Giraudet[a], M.C. Schouler[b], P. Gadelle[b], A. Hamwi[a]

[a]*Laboratoire des Matériaux Inorganiques, UMR CNRS 6002-Université B. Pascal, 24 av. des Landais, 63177 Aubière Cedex, France*
[b]*Laboratoire de Thermodynamique et de Physico-Chimie Métallurgiques, CNRS-INPG-Université J. Fourier, BP 75,
38402 Saint Martin d'Hères Cedex, France*

Abstract

The reactivity of multiwall carbon nanotubes toward WF_6, a strong Lewis acid, has been studied. A material of nominal composition $C_{36}WF_6$ has been obtained and characterized by X-ray diffraction. Intercalation between pseudo-graphitic layers has been evidenced, leading to a staging phenomenon at the nanometer scale. A structural model is proposed and the intercalation chemistry of multiwalled carbon nanotubes is discussed.
© 2004 Elsevier Ltd. All rights reserved.

PACS: 61.10 Nz; 61.48 tc; 61.46 tw

Keywords: A. Carbon nanotubes; A. Inorganic fluorides; B. Intercalation

1. Introduction

Much work has been devoted to the properly speaking chemistry of carbon nanotubes, including their synthesis, purification and chemical reactivity with various compounds. Thus, the covalent chemistry of carbon nanotubes parallels the functionalization of graphite and halogenated [1,2], oxygenated [3,4] or alkylated [5] derivatives, have been obtained. The analogy between the chemical properties of carbon nanotubes and those of the latter well-known allotropic form of carbon also extends to intercalation chemistry, within a somehow more general frame, due to the particular dimensionality of the host–lattice in this case. Thus, many examples of a reversible filling of the central channel by capillarity have been reported in the literature [6–11]. The illustration can be further extended by considering the special case of some particular carbon nanotubes, consisting in one single rolled up graphitic layer,

ordered in a close-packed lattice of cylinders, i.e. the so-called bundle of single-wall nanotubes. The occupation of the corresponding intertubular van der Waals gap by different kinds of guest-species is also well documented [12–20]. The last and more conventional situation encountered involves the available interlayer space inherent to the regular stacking of concentric graphene layers constituting a multiwalled carbon nanotube (MWNT). Though the opportunity of accommodation of intercalated species at this level of the structure turns out to be a pertinent concept, few attention has been paid to the latter and much work remains to be done in this field. Hence, only the chemical doping of MWNTs with some alkali metals [21–28] and a few transition metal halides [22,23,29] seems to have been reported, so far. While most of these earlier studies [24–28] focused on the electrochemical energy storage for a potential use of carbon nanotubes in Li-ion batteries, a detailed description of the lattice properties at the atomic level of the MWNT-based intercalation compounds has never really been explicit. However, some aspects inherent to the effect of an intercalation/de-intercalation process on the overall morphology of a MWNT have already been depicted [21–24].

* Corresponding author. Tel.: +33-473-407-647; fax: +33-473-407-108.

E-mail address: claves@chimtp.univ-bpclermont.fr (D. Claves).

We will therein present results concerning the reactivity of WF_6 toward MWNTs. The latter inorganic fluoride, well known to readily intercalate graphite as an electron acceptor, may be the source of a prototypical p-type doped carbon nanostructure. We will show that the structural order in the new material obtained can be described in terms of a 'nanostaging' phenomenon.

2. Experimental

2.1. Synthesis and purification of the MWNTs

MWNTs were prepared via a catalytic method, previously described in Ref. [30] and involving the disproportionation, at 510 °C, of carbon monoxide (Boudouard reaction) over alumina-supported Co catalyst particles.

In order to avoid the formation of oxygenated addends at the outer surface, a two-step purification method was employed, involving relatively soft conditions. An oxidation treatment in air at moderated temperature was first applied (450 °C, 20 min), followed by a chemical treatment with a concentrated HF–HCl mixture (50/50% in volume). The temperature of 450 °C used in the first step was optimized by thermogravimetric analysis (TGA) and corresponds to the starting point of decomposition in air of our MWNTs.

2.2. WF_6 elaboration and intercalation conditions

Tungsten hexafluoride was prepared in a first reactor by direct reaction of a pure fluorine atmosphere with the metal, heated at 300 °C. In order to increase the reaction rate, the MWNTs were put in a secondary reactor, cooled at -20 °C with a salt–ice bath and connected to the main reactor, so that the gaseous fluoride condense at this level. The container was then isolated and placed at room temperature for 24 h.

2.3. Characterization

The starting MWNTs were characterized by transmission electron microscopy (TEM) with a Jeol microscope operating at 200 kV

TGA were performed in air on raw and purified MWNTs using a Shimadzu TGA-50, with a heating rate of 2 °C/min.

Samples of pristine MWNTs and of the MWNTs–WF_6 material were conditioned in 0.5 mm diameter sealed capillaries. Powder X-ray diffraction measurements were performed using a Philips X'Pert Pro diffractometer, working with the Cu Kα1 radiation. Diffraction patterns were collected in the transmission mode with a position sensitive detector.

3. Results

A batch of MWNTs was synthesized and further purified as described in Section 2. A structural study being facilitated by the presence of an appreciable coherence length in the material, the average final number of graphene layers was, therefore, modulated in this sense.

The TEM observations (Fig. 1(a)–(c)) confirm the quasi total removal of residual alumina and cobalt particles after the purification process and the effective opening of a significant part of the initially end-capped nanotubes. The inner diameter distribution of the MWNTs remains narrow and the number of layers seems to be in the vicinity of 15 for most of the tubes (Fig. 1).

The distribution of interlayer spacing, obtained from the position of the main line in the diffraction pattern (Fig. 2), which is equivalent to the (002) reflection of graphite, is centred on 0.342 nm. The average coherence length, extrapolated from the FWHM of such a Bragg peak, in which the finite-size effect contribution to the global profile is supposed to be largely predominant, corresponds to 15 successive stacked layers, in agreement with the HRTEM observations. Though X-ray diffraction also shows that the purification technique employed is suitable to obtain MWNTs with correct purity, the persistence of some small amplitude signals arising from residual Co catalytic particles remains visible. In the conditions used, the average carbon thickness at the tips appears then sufficient to partly resist the preliminary oxidative treatment in air and, thereby, hinders a complete opening of all tubes. Some of the metal particles, located at the extremities and still embedded in a carbon coating, remain isolated from the subsequent acid wash and are not eliminated. However, a complementary TGA up to 600 °C in air, during which only carbon is consumed, shows that the relative amount of carbon is more than 99% after purification and in regard to the forthcoming structural investigation, such impurity traces are not bothersome.

After exposure of the MWNTs to the gaseous reagent vapours, according to the aforementioned experimental procedure, the nominal composition of the reaction product, determined by weight uptake (within ± 0.5 mg), is $C_{36\pm3}WF_6$. It can consequently be noticed that the accommodation of fluoride into the carbon matrix remains low, compared to graphite powder in similar conditions for which a ratio C/W = 18 can be easily reached [32].

The relevant diffraction pattern (Fig. 2) exhibits a single dominant Bragg peak, characteristic of some raw MWNTs or of longitudinal sections remaining unaffected, and apart from the emergence of a broad shoulder beside this initial main line, the diffraction data are not sensibly modified. The latter additional feature observed has been interpreted in terms of a novel 'long range' order in the material, related to an effective intercalation process. Since a precise determination of each angular position turns out to be delicate, due to the poorly resolved signals, the structural analysis of the
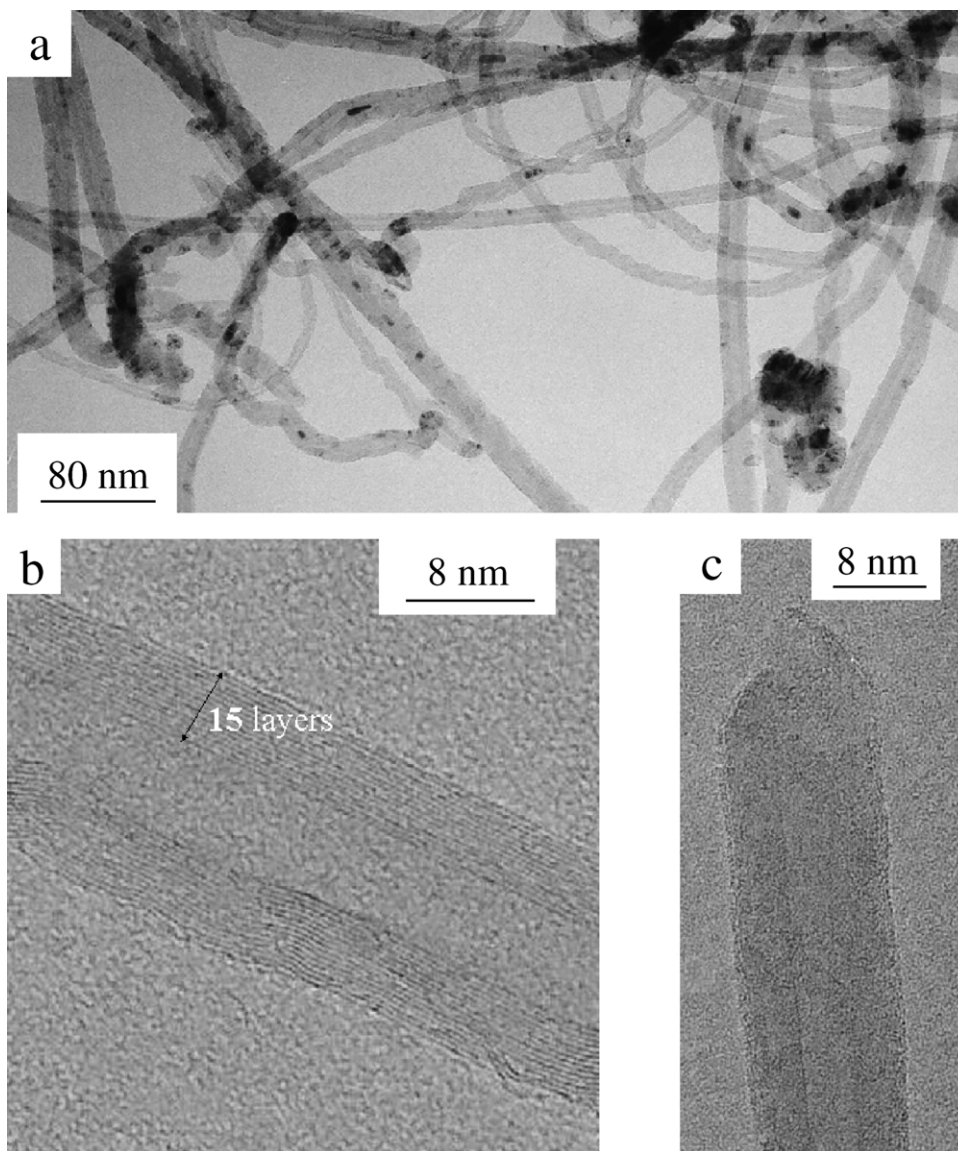
Fig. 1. Transmission electron micrographs of purified MWNTs, produced by thermal decomposition of CO over Co catalyst, showing (a) some individual tubes in the sample, (b) the layers organization in a tube and (c) the effective opening of some tubes and removal of cobalt particles at the tips.

intercalated phase can consequently not be performed without reference to a pre-existing model.

The diffraction pattern has then tentatively been analysed from the hypothesis stipulating the presence, beside the raw material, of a major stage number associated with the intercalated part of the sample and on the basis of an analogy with the reflections issuing from the graphite–fluorides intercalation compounds (GICs) [31–35], among which (001) lines are largely prominent as a signature of the lamellar character of these phases. Thus, the structurally constrained model used here considers a one-dimensional statistically disordered atomic distribution along the stack-ing direction of the curved carbon layers. The intercalated phase is assigned an arbitrary stage number N, with a corresponding identity period along the previous axis, $I_c = Nd_0 + t$, where $d_0 = 0.342$ nm is the distance between adjacent shells in the pristine carbonaceous material and t is the thickness of the intercalate. The latter can be given the value 0.49 nm, by referring to the c-axis parameters reported for homologous WF_6-based GICs formed under similar synthesis conditions [32]. The orientation of the intercalated species should be suitable with the realization of the most compact atomic arrangement and with the optimization of the carbon–fluorine interactions, by putting as many
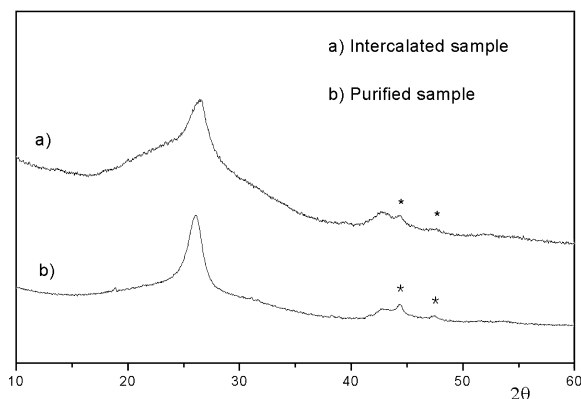
Fig. 2. X-ray diffraction patterns of the pristine and intercalated MWNTs ($*$ denote reflections from some residual Co particles).

fluorine atoms as possible in contact with the carbon sheets. Thus, for an hexacoordinated atom $t = 2L/\sqrt{3} + 2R_F$, where $L = 0.1832$ nm is the W–F bond length [36] and R_F represents an ad-hoc radius for the fluorine atoms satisfying the above relation and accounting for some possible distortions from a regular octahedron. The resulting average atomic coordinates used are detailed in inset on Fig. 3.

The angular range explored has been restricted to the only zone where significant modifications are observed in the pattern and extends over $2\theta = 10-40°$, which allows to consider a constant peak width for the deconvolution. At this stage, a standard least-squares fit procedure can then be applied to refine the peak shape parameters and the C/WF$_6$ ratio. The best fit has been obtained for a stage 4 (supposed largely predominant) model and a related composition C$_{34}$WF$_6$. The satisfying matching of the corresponding extracted intensities to experimental data is shown in Fig. 3.
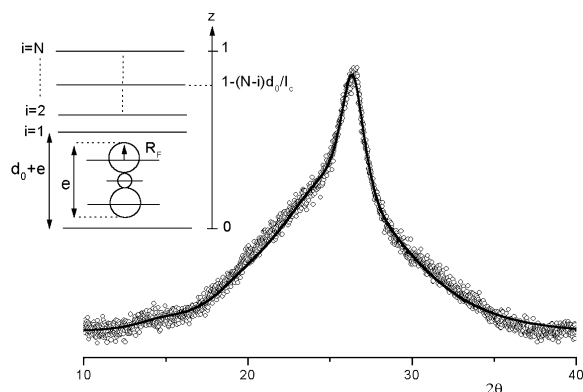

Fig. 3. X-ray diffraction pattern in the low angle region and after background subtraction of the MWNTs-WF$_6$ sample. Dots are experimental data and line is the refined profile obtained from a stage 4 structural scheme with optimized parametrization. Inset provides details on the fractional atomic coordinates system used for the intercalated phase (all symbols refer to text).

4. Discussion

The admixture of unreacted MWNTs in the sample or the presence of non-intercalated zones along the tube axis gives evidence, since the global experimental composition and the refined composition of the intercalated phase are similar, that part of the fluorinated molecules are involved in competing fixation modes to the carbon substrate. Adsorption at the outer surface, condensation in the central channel or trapping at local defects sites (edges) are, therefore, highly probable and cannot be evidenced by XRD.

The FWHM of the broad X-ray signature of the intercalated domain, determined from the previous refinement, allows to specify that the size of the latter is equivalent to one single unit cell in thickness (~ 2 nm) and that consequently, the staging sequence observed is in no way a bulk property of the system but remains a surface phenomenon. The former conclusion seems to be indirectly confirmed by the HRTEM observations (Fig. 1(b)) which show discontinuous carbon shells near the outer surface of the tubes. Indeed, the presence of such wall disjunctions turns out to be necessary for an intercalation mechanism to be possible, since the increase in the carbon layers separation which results could not occur from an organization of nested closed cylinders. This fact supports the limitation of fluoride intercalation near the surface only, where such pre-existing defects are present.

The aforementioned mechanistic approach of insertion phenomena in such a medium is not without importance in regard to further elaboration of CNT-based intercalation compounds. The relative abundance of local defects observed in the pristine MWNTs used in this work outlines the advantage of the catalytic synthesis process retained, which manifestly favors the formation of the necessary structural disorder in the stacking of the curved graphene sheets. Catalytically grown MWNTs elaborated at low temperature appear, therefore, as privileged precursors to be exploited in the formation of low dimensional intercalation compounds of and of their subsequent derivatives.

A last comment may be added concerning the effective global morphology of the final intercalated product, in relation with the persistence of the raw CNT signal in the diffraction pattern. The direct observation of an intercalated tube is extensively difficult here, owing to rapid de-intercalation of the volatile halide in a vacuum chamber. Somehow, rather than the unlikely presence in the sample of tubes either selectively non-intercalated or completely intercalated over their whole length, and complying with earlier microscopy observations [22–24] of a heterogeneous swelling of doped MWNTs, it seems more advisable to infer a successive alternation of intercalated and non-intercalated sections along the longitudinal axis of each tube. An organization of locally non-closed and superposed graphitic fragments alternating with non-intercalable perfectly nested shells seems to be the only configuration allowing to

account for a partial and sequential insertion process along the tube axis.

5. Conclusion

The intercalation chemistry of MWNTs is gaining credence for it may find practical applications in electrochemical energy storage (Li, H_2…) or supported catalysis. The main interest of the resulting nanometer scale edifices may also lie in the perspectives they offer toward the elaboration of nanostructured materials by allowing to confine, in their tubular interlayer space, a chemical reaction between two preliminary intercalated species, as recently reported for some GICs' [35]. After easy elimination of the carbon template, the morphological imprint of the initial matrix should be maintained.

References

[1] A. Hamwi, H. Alvergnat, S. Bonnamy, F. Béguin, Carbon 35 (6) (1997) 723.

[2] E.T. Mickelson, C.B. Huffman, A.G. Rinzler, R.E. Smalley, R.H. Hauge, J.L. Margrave, Chem. Phys. Lett. 296 (1998) 188.

[3] H. Ago, T. Kugler, F. Cacialli, W.R. Salaneck, M.S.P. Shaffer, A.H. Windle, R.H. Friend, J. Phys. Chem. B 103 (1999) 8116.

[4] K.C. Hwang, J. Chem. Soc., Chem. Commun. (1995) 173.

[5] P.J. Boul, J. Liu, E.T. Mickelson, C.B. Huffman, L.M. Ericson, I.W. Chiang, K.A. Smith, D.T. Colbert, R.H. Hauge, J.L. Margrave, R.E. Smalley, Chem. Phys. Lett. 310 (1999) 367.

[6] P.M. Ajayan, S. Iijima, Nature 361 (1993) 333.

[7] S.C. Tang, Y.K. Chen, P.J.F. Harris, M.L.H. Green, Nature 372 (1994) 159.

[8] D. Ugarte, A. Châtelain, W.A. de Heer, Science 274 (1996) 1897.

[9] J. Sloan, J. Cook, A. Chu, M. Zwiefka-Sibley, M.L.H. green, J.L. Hutchinson, J. Solid State Chem. 140 (1998) 83.

[10] C.H. Kiang, J.S. Choi, T.T. Tran, A.D. Bacher, J. Phys. Chem. B 103 (1999) 7449.

[11] J. Mittal, M. Monthioux, H. Allouche, O. Stephan, Chem. Phys. Lett. 339 (2001) 311.

[12] R.S. Lee, H.J. Kim, J.E. Fisher, A. Thess, R.E. Smalley, Nature 388 (1997) 255.

[13] C. Bower, S. Suzuki, K. Tanigaki, O. Zhou, Appl. Phys. A 67 (1998) 47.

[14] A.S. Claye, J.E. Fisher, C.B. Huffman, A.G. Rinzler, R.E. Smalley, J. Electrochem. Soc. 147 (8) (2000) 2845.

[15] B. Gao, A. Kleinhammes, X.P. Tang, C. Bower, L. Fleming, Y. Wu, O. Zhou, Chem. Phys. Lett. 307 (1999) 153.

[16] S. Suzuki, C. Bower, O. Zhou, Chem. Phys. Lett. 285 (1998) 230.

[17] L. Grigorian, G.U. Sumanasekera, A.L. Loper, S. Fang, J.L. Allen, P.C. Eklund, Phys. Rev. B 58 (8) (1998) R4195.

[18] A.S. Claye, N.M. Nemes, A. Janossy, J.E. Fisher, Phys. Rev. B 62 (8) (2000) R4845.

[19] G.U. Sumanasekera, J.L. Allen, S.L. Fang, A.L. Loper, A.M. Rao, P.C. Eklund, J. Phys. Chem. B 103 (1999) 4292.

[20] C. Bower, A. Kleinhammes, Y. Wu, O. Zhou, Chem. Phys. Lett. 288 (1998) 481.

[21] O. Zhou, R.M. Fleming, D.W. Murphy, C.H. Chen, R.C. Haddon, A.P. Ramirez, S.H. Glarum, Science 263 (1994) 1744.

[22] V.Z. Mordkovich, M. Baxendale, S. Yoshimura, R.P.H. Chang, Carbon 34 (1996) 1301.

[23] V.Z. Mordkovich, Mol. Cryst. Liq. Cryst. 340 (2000) 775.

[24] G. Maurin, Ch. Bousquet, F. Henn, P. Bernier, R. Almairac, B. Simon, Chem. Phys. Lett. 312 (1999) 14.

[25] E. Frackowiak, S. Gautier, H. Gaucher, S. Bonnamy, F. Béguin, Carbon 37 (1999) 61.

[26] F. Leroux, K. Méténier, S. Gautier, E. Frackowiak, S. Bonnamy, F. Béguin, J. Power Sources 81–82 (1999) 317.

[27] G. Maurin, Ch. Bousquet, F. Henn, P. Bernier, R. Almairac, B. Simon, Solid Sate Ionics 136–137 (2000) 1295.

[28] Z. Yang, H. Wu, Solid State Ionics 143 (2001) 173.

[29] J. Giraudet, M. Dubois, D. Claves, J.P. Pinheiro, M.C. Schouler, P. Gadelle, A. Hamwi, Chem. Phys. Lett. 381 (2003) 306.

[30] J.P. Pinheiro, M.C. Schouler, P. Gadelle, M. Mermoux, E. Dooryhée, Carbon 38 (10) (2000) 1469.

[31] A. Hamwi, Ph. Touzain, L. Bonnetain, Mater. Sci. Engng 31 (1977) 95.

[32] S. Mouras, A. Hamwi, D. Djurado, J.C. Cousseins, Rev. Chim. Miner. 24 (5) (1987) 572.

[33] R. Yazami, T. Nakajima, Synth. Met. 34 (1989) 109.

[34] A. Hamwi, D. Claves, A. Senhaji, J. Fluorine Chem. 110 (2001) 153.

[35] J. Giraudet, D. Claves, A. Hamwi, Synth. Met. 118 (2001) 57.

[36] J.H. Canterford, R. Carlton, Halides of the Second and Third Row Transition Metals, Wiley, New York, 1969.